AIDA-2020-CONF-2019-005

AIDA-2020

Advanced European Infrastructures for Detectors at Accelerators

Conference/Workshop Paper

Gain Stabilization of SiPMs and Afterpulsing

Eigen, G. (University of Bergen) *et al*

22 May 2018

The AIDA-2020 Advanced European Infrastructures for Detectors at Accelerators project has received funding from the European Union's Horizon 2020 Research and Innovation programme under Grant Agreement no. 654168.

This work is part of AIDA-2020 Work Package **14: Infrastructure for advanced calorimeters**.

The electronic version of this AIDA-2020 Publication is available via the AIDA-2020 web site <http://aida2020.web.cern.ch> or on the CERN Document Server at the following URL: <http://cds.cern.ch/search?p=AIDA-2020-CONF-2019-005>

Gain Stabilization of SiPMs and Afterpulsing

Gerald Eigen

Department of Physics and Technology, University of Bergen, N-5007 Bergen, NORWAY ‡

E-mail: gerald.eigen@ift.uib.no

July 2018

Abstract. The gain of silicon photomultipliers increases with bias voltage and decreases with temperature. To operate SiPMs at stable gain, the bias voltage can be readjusted to compensate for temperature changes. We have tested this concept with 30 SiPMs from three manufacturers in a climate chamber at CERN varying the temperature from 1°C to 48°C. We built an adaptive power supply that is based on a linear dependence of bias voltage versus temperature. With one selected dV_b/dT value, we stabilized four SiPMs simultaneously. We fulfilled our goal of stabilizing most SiPMs with gain changes of less than 0.5% in the $20° - 30°$C temperature range. We studied afterpulsing of SiPMs for different temperatures and bias voltages.

1. Introduction

The gain of silicon photomultipliers (SiPMs) [1, 2, 3] increases with bias voltage V_b and decreases with temperature T. We achieve stable gain by readjusting the bias voltage appropriately if the temperature changes. This procedure requires detailed knowledge of dV_b/dT. We define stable gain as a gain change $\Delta G \leq \pm 0.5\%$ in the $20° - 30°$C temperature range. We have tested this procedure with 30 SiPMs (18 from Hamamatsu, eight from KETEK and four from CPTA) using a custom-made adaptive power supply that accomplishes automatic linear dV_b/dT adjustments when the temperature changes. Automatic gain stabilization is particularly important for the operation of large detector system like an analog hadron calorimeter [4].

2. Experimental Setup

We performed all gain stabilization studies in a climate chamber at CERN. Figure 1a shows the experimental setup in which we simultaneously test four SiPMs that are housed in separate compartments inside a black box to prevent optical cross talk. Each SiPM is read out with a two-stage preamplifier. A digital oscilloscope with four 12-bit

‡ on behalf of G. Eigen, A. Tret, J. Zalieckas (Bergen U.), J. Cvach, J. Kvasnicka, I. Polak (Prague, Inst. Phys., CAS)

ADCs (LeCroy HDO6104) processed the amplified signals at a rate of 5 Mb/s. We illuminated each SiPM with blue LED light. To minimize noise pickup, we placed the LEDs outside the climate chamber and transported the LED light via clear fibers to each SiPM. We adjusted the intensity such that in addition to a clearly visible pedestal several photoelectron peaks were produced. We recorded 50000 waveforms per run. Figure 1b shows waveforms and photoelectron spectra for Hamamatsu SiPMs S13360, which have trenches to reduce the pixel-to-pixel cross talk. Individual photoelectron peaks are clearly visible on the waveforms. We recorded the temperature with seven sensors, placing one close to each SiPM. While we illuminated the surface of Hamamatsu and KETEK SiPMs directly, this was not possible for CPTA sensors, since they were glued to a wavelength-shifting fiber housed in a groove in a scintillator tile. To reach the SiPM surface the LED light had to be absorbed and re-emitted in the wavelength-shifting fiber.

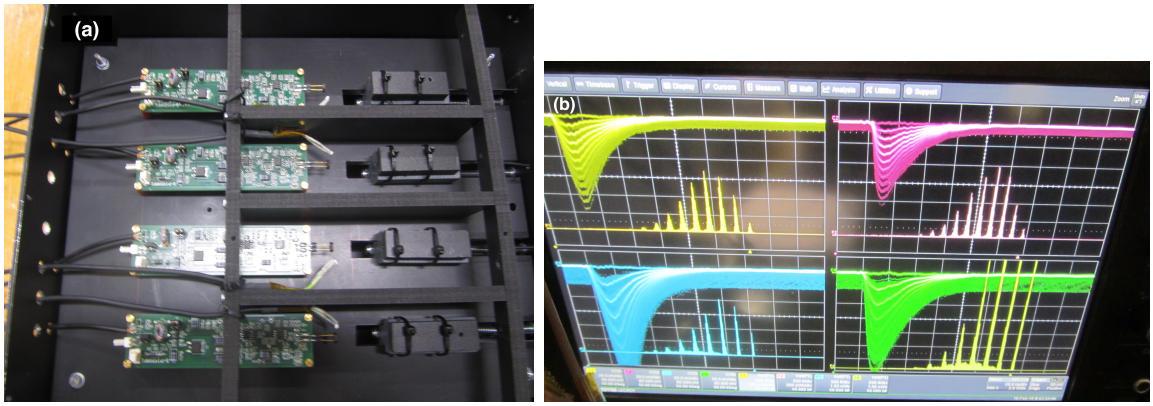

Figure 1. (a) Setup of the gain stabilization measurements inside a black box. The green circuit boards host preamplifiers and signal readout. The black cable at the left end of the board is the signal cable. Each SiPM is inserted into a connector on the right end of the board. One temperature sensor is placed near each SiPM. Clear fibers transporting blue LED light run inside the black distance-adjustable foam boxes on the right. (b) Waveform and photoelectron spectra of four Hamamatsu S13360 SiPMs.

3. Gain measurements

After subtracting a parasitic pick-up noise caused by a defect cable, we integrated the waveforms over a variable time window. The start time is set to the beginning of the waveform and the stop time is defined as the time when the signal reaches the baseline again. This produced stable photoelectron spectra for all Hamamatsu SiPMs. However, for KETEK and CPTA SiPMs this method did not succeed for all values of V_b and T. Therefore, we extracted the photoelectron spectra from the minimum of the waveform, which always produced photoelectron spectra with clearly visible first and second photoelectron peaks. [5]. The gain is defined as the distance between the second and first photoelectron peaks, which is the same as the distance between first

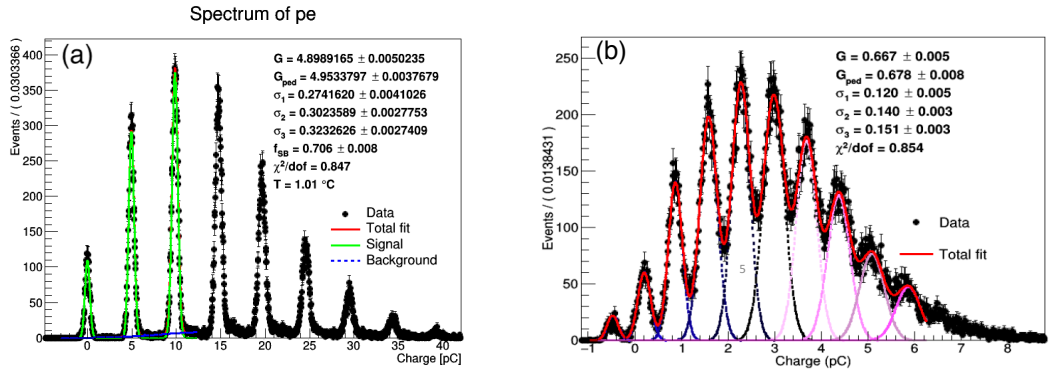

Figure 2. (a) Photoelectron spectrum of Hamamatsu SiPM with trenches with results of the first fit model overlaid; (b) Photoelectron spectrum of Hamamatsu SiPM without trenches with results of the second signal model overlaid. The gain is the difference between second and first photoelectron peaks.

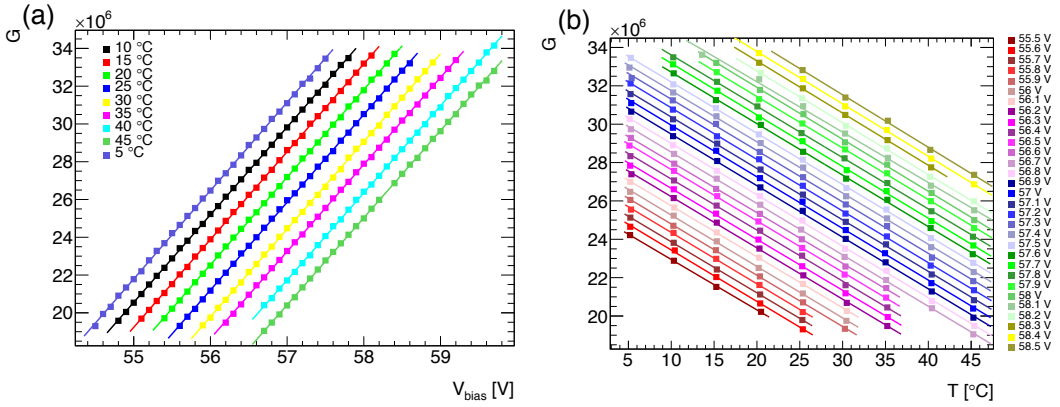

Figure 3. (a) Measurements of gain (points) versus bias voltage at different temperatures for a Hamamatsu MPPC S13360-1325 with fit results overlaid (solid lines). (b) Measurements of gain (points) versus temperature for different bias voltages for a Hamamatsu MPPC S13360-1325 with fit results overlaid (solid lines).

photoelectron peak and pedestal. We chose this definition for historic reasons since in a previous setup the pedestal was not always recorded. We use two methods to fit photoelectron spectra. In the first method, we fit the first and second photoelectron peaks in addition to the pedestal plus a small background that is determined by a sensitive nonlinear iterative peak-clipping algorithm (SNIP) available in ROOT [6] (see Fig. 2a). Positions, widths and fractions of the Gaussian functions are free parameters in the fit. In the second method, we fit all visible photoelectron peaks and the pedestal with individual Gaussians keeping all widths and fractions as free parameters (see Fig. 2b). For each SiPM, we first determine dV_b/dT by performing a two-dimensional fit of gain measurements as functions of bias voltage and temperature.

$$G(V_\mathrm{b}, T) = G_0 + \frac{dG}{dV_\mathrm{b}} * (V_\mathrm{b} - V_0) + \frac{dG}{dV_\mathrm{b}} * \frac{dV_\mathrm{b}}{dT} * (T - T_0),$$

where G_0, dG/dV_b and dV_b/dT are extracted from the fit. Figures 3a,b show the gain

dependence versus $V_{\rm b}$ and T, respectively. Using a common $dV_{\rm b}/dT$ compensation value we tested gain stabilization of four SiPMs simultaneously.

4. Gain Stabilization Studies

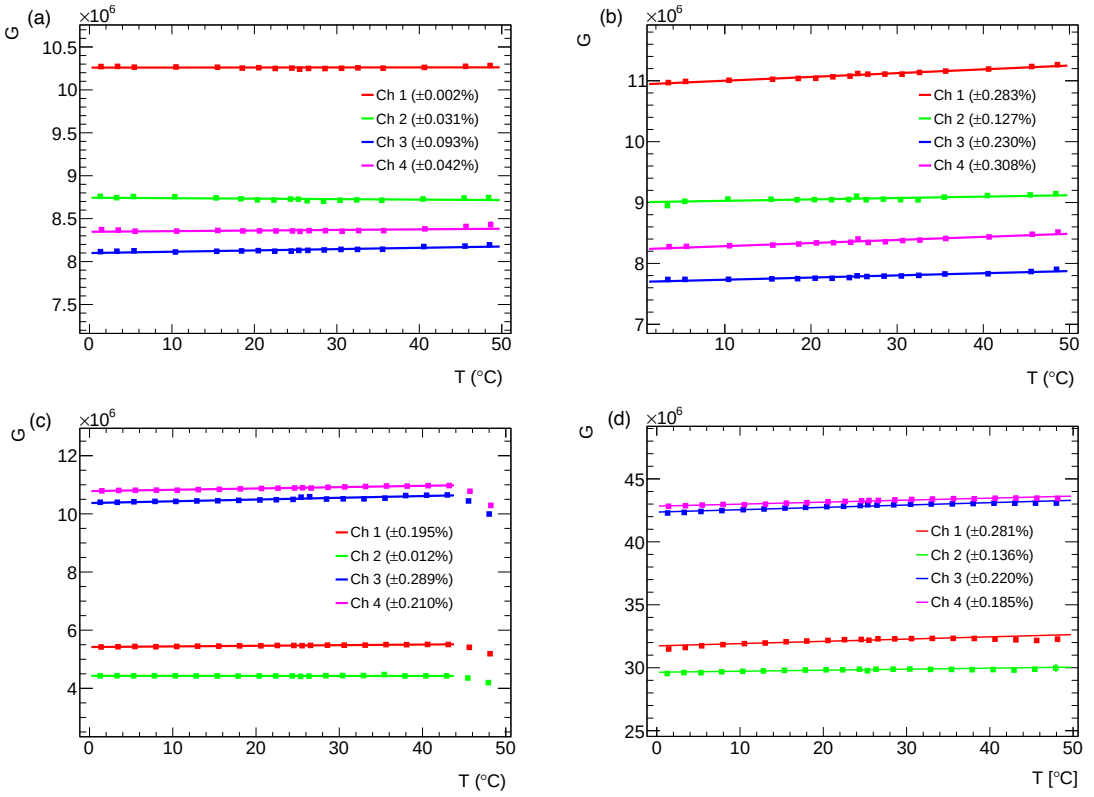

Figure 4. Measurements of gain versus temperature with fit results overlaid. (a) all A-type sensors; (b) all B-type sensors; (c) all S12571 sensors; (d) all S13360 sensors. The A-type, B-type and S12571 sensors have no trenches while S13360 sensors have trenches. We use the first (second) fit models for SiPMs with (without) trenches.

Selecting one compensation value $dV_{\rm b}/dT$ for four SiPMs, we performed the stabilization tests overnight with the bias voltage regulator board [7]. We varied the temperature from typically from 48°C to 1°C in steps of ~ 2.5°C except for the $20°-30$°C range where the step size was reduced to ~ 2.0°C. Since the temperature stabilized after 15 minutes, we stayed at each temperature point for 30 minutes to record at least 18 runs with 50000 waveforms each at stabile temperature. We first tested 18 SiPMs from Hamamatsu [8]. The nominal bias voltage for sensors without trenches lies around 65-75 V while that for sensors with trenches lies around 50-60 V.

Figure 4 shows the gain stabilization results for Hamamatsu A-sensors (a), B-sensors (b), S12571 sensors (c) and S13360 sensors (d). Table 1 summarizes the deviation from uniformity in the $20° - 30$°C temperature range. All Hamamatsu SiPMs satisfy our criteria of $\Delta G/G < 0.5\%$. Several Hamamatsu SiPMs actually satisfy this criterion in the fully tested temperature range.

Table 1. Measured gain deviations $\Delta G/G$ from uniformity in the $20-30°$C temperature range.

SiPM	set dV_b/dT [mV/°C]	Ch1 $\Delta G/G$	Ch2 $\Delta G/G$	Ch3 $\Delta G/G$	Ch4 $\Delta G/G$
Hamamatsu A	59.0	A1-20 $\pm$ **0.002**%	A2-20 $\pm$**0.031**%	A2-15 $\pm$**0.093**%	A1-15 $\pm$**0.042**%
Hamamatsu B	58.0	B1-20 $\pm$**0.283**%	B2-20 $\pm$**0.127**%	B2-15 $\pm$**0.230**%	B1-15 $\pm$**0.308**%
Hamamatsu S12571-	64.8	010-271 $\pm$**0.195**%	010-273 $\pm$**0.012**%	015-137 $\pm$**0.289**%	015-136 $\pm$**0.0210**%
Hamamatsu S13360-	57.0	1325-10143 $\pm$**0.281**%	1325-10144 $\pm$**0.136**%	3025-10104 $\pm$**0.220**%	3025-10103 $\pm$**0.185**%
Hamamatsu S13360-	57.2	1325-10143 $\pm$**0.151**%	1325-10144 $\pm$**0.05**%	LCT4#6 $\pm$**0.051**%	LCT4#9 $\pm$**0.045**%
KETEK W12/PM3350	18.2	W12-A $\pm$**0.59**%	W12-B $\pm$**0.79**%	PM3350-1 $\pm$**1.62**%	PM3350-2 $\pm$**1.43**%
KETEK PM3350	18.2	PM3350-5 $\pm$**1.41**%	PM3350-6 $\pm$**1.39**%	PM3350-7 $\pm$**1.65**%	PM3350-8 $\pm$**1.64**%
CPTA	21.2	#857 $\pm$**0.017**%	#922 $\pm$**0.307**%	#975 $\pm$**0.161**%	#1065 $\pm$**0.032**%

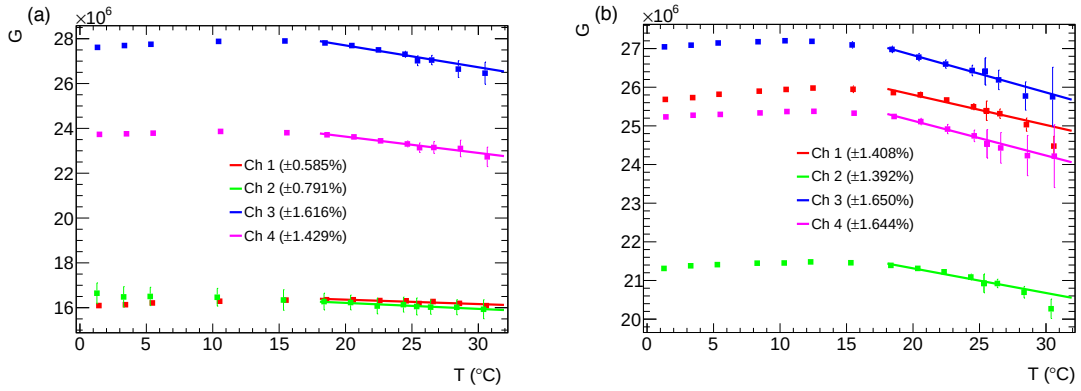

Figure 5. Measurements of gain versus temperature. (a) W12A, W12B, PM3350#1 and PM3350#2 sensors; (b) four PM3350 sensors (#5 to #8).

We tested eight SiPMs from KETEK [9]. The nominal bias voltage is around 28 V. Since the decay time of KETEK SiPM waveform is much longer than that of Hamamatsu SiPMs the waveform typically does not return to the baseline within 200 ns. We, therefore, extract the SiPM photoelectron spectrum from the minimum position of the waveform. The KETEK SiPMs do not work properly at temperatures above 30°C. Figure 5a,b show the gain versus temperature dependence after stabilization. The KETEK sensors show a more complicated $V(T)$ dependence. A linear gain compensation

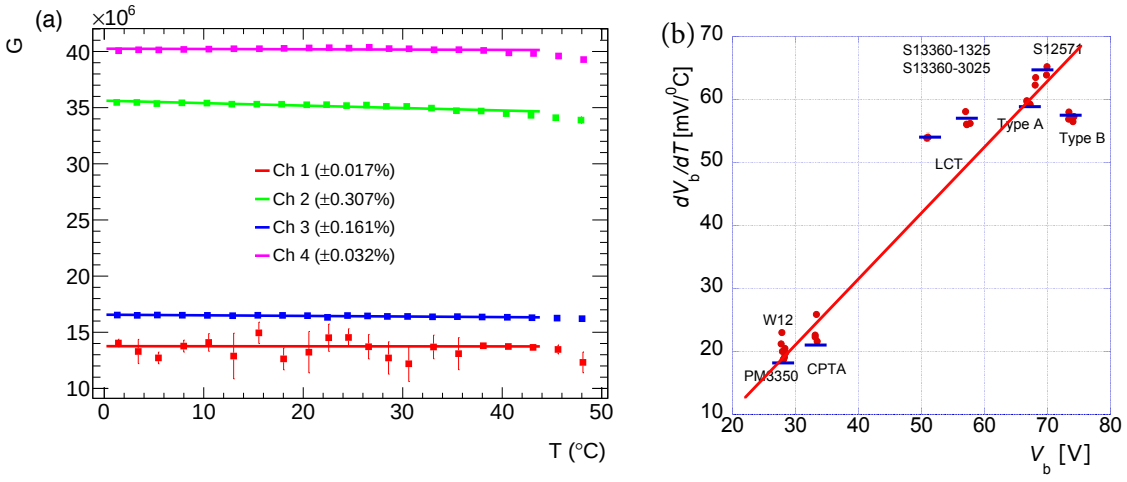

Figure 6. (a) Measurements of gain versus temperature for CPTA sensors #857, #922, #975 and #1065. (b) Correlation of $dV_{\rm b}/dT$ versus bias voltage. Except for some experimental devices the linearity between $dV_{\rm b}/dT$ and $V_{\rm b}$ works well.

is not sufficient. For low temperatures ($1^\circ - 18^\circ$C) the gain rises slowly remaining constant in the range $18^\circ - 22^\circ$C before declining again. Table 1 summarizes the results. No SiPM satisfies our gain stability criterion.

The CPTA SiPMs operate in the full $1^\circ - 48^\circ$C temperature range [10]. Figure 6 shows the gain stabilization results. The gain is nearly uniform up to 30°C. The operation of SiPMs #922 and #1065 look fine; SiPM #857 was rather noisy and SiPM #975 changed gain after operation at $T = 45^\circ$C but worked fine afterwards. All CPTA SiPMs satisfy our gain stability criterion. Table 1 summarizes our results of linear deviation from uniformity in the $20^\circ - 30^\circ$C temperature range.

5. Afterpulsing Effects

We developed two procedures to extract the photoelectron spectra from the measured waveforms, either by integrating the charge over a variable time window or from evaluating the maximal amplitude of the waveform at its minimum. The former is sensitive to contributions from afterpulsing while the latter is typically not. Thus, we can determine the amount of afterpulsing from the scatter plot of charge versus maximum amplitude shown in Fig. 7a. The red elliptical spots show the individual photoelectron peaks without afterpulsing contributions lying on the diagonal. For waveforms with afterpulsing contributions, the charge is shifted vertically since the waveform is broadened by the delayed second signal producing small satellite peaks separated from the peaks without afterpulsing by a valley as shown in Fig. 7b. The dashed line shows the separation of waveforms with afterpulsing from those without. The slope $a = \Delta y/\Delta x$ is calculated from the separations $(\Delta x, \Delta y)$ of the three-photoelectron peak from the two-photoelectron peak in the maximum amplitude and charge observables, respectively.

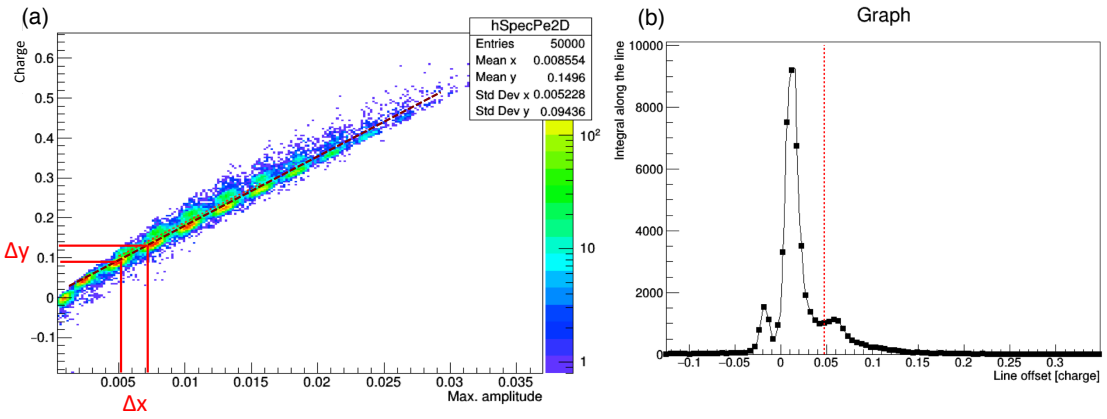

Figure 7. (a) Scatter plot of integrated charge versus maximum amplitude at waveform minimum and (b) the projection orthogonal to the dashed line. The peak represents all contributions of photoelectron peaks that are not affected by afterpulsing while the small peak to the right shows photoelectron peaks affected by afterpulsing.

If we select only waveforms that lie below the dashed line we obtain a sample with reduced afterpulsing. Stabilization tests for this sample agree well with those of the full sample. This demonstrates that afterpulsing has no effect on gain stabilization. We define the ratio R of afterpulse waveforms lying above the red dashed line in Fig. 7 to all entries and study R versus V_b and T. Figures 8a, b show R versus V_b for different temperatures for both LCT SiPMs. The fraction of afterpulse waveforms increases strongly with overvoltage $\Delta V = V_\mathrm{b} - V_\mathrm{break}$. For $\Delta V = 1$ V, R is less than 1% while for $\Delta V = 4$ V, R increase to $> 30\%$. We observe no explicit temperature dependence. The spread in the different curves indicates the systematic effect of the procedure.

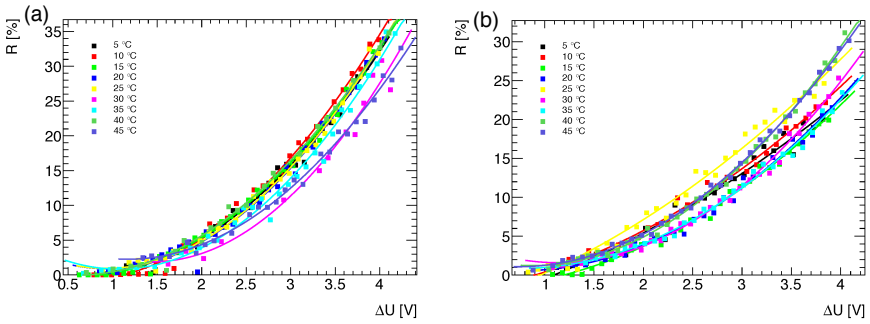

Figure 8. The fraction of aflerpulse waveforms as a function of overvoltage for different temperatures for LCT4#6 (a) and LCT4#9 (b).

6. Conclusions

We successfully completed gain stabilization tests for 30 SiPMs demonstrating that batches of SiPMs can be stabilized with one compensation value of dV_b/dT. All 18

Hamamatsu SiPMs satisfy our stabilization criterion, most of them even satisfy this in the extended temperature range of $1^\circ - 48^\circ$C. Gain stabilization of KETEK SiPMs is more complicated since the signals are rather long and are affected by afterpulsing. The temperature range is limited to $1^\circ - 30^\circ$C. We did not succeed in stabilizing any of the eight KETEK SiPMs tested. The $V(T)$ dependence seems to be more complicated being non linear. Gain stabilization of CPTA SiPMs works well. All four SiPMs satisfy our criterion. In the analog HCAL for ILC, the bias voltage adjustment will be implemented on the electronics boards. Gain stabilization looks promising if the temperature is well measured and SiPM with similar properties are stabilized with one dV_b/dT compensation value. Afterpulsing depends on the bias voltage but has no effect on gain stabilization.

7. Acknowledgments

This work was conducted in the framework of the European network AIDA2020. It has been supported by the Norwegian Research Council and by the Ministry of Education, Youth and Sports of the Czech Republic under the project LG14033.We would like to thank L. Linssen, Ch. Joram, W. Klempt, and D. Dannheim for using the E-lab and for supplying electronic equipment. We further would like to thank the team of the climate chamber at CERN for their assistance and support.

8. References

[1] G. Bondarenko el al., Nucl. Instrum. Meth. **A** 442, 187 (2000).
[2] P. Buzhan el al., Proceedings of the 7th Int. Conf. on Advanced Technology and Particle Physics, 717 (2002).
[3] P. Buzhan el al., Nucl. Instrum. Meth. **A** 504, 48 (2003).
[4] CALICE collaboration (C. Adloff et al.), *Construction and Commissioning of the CALICE Analog Hadron Calorimeter Prototype*, JINST **5**, P05004 (2010).
[5] G. Eigen *et al.*, SiPM Gain Stabilization for Adaptive Power Supply, article in JINST in preparation (2018).
[6] R. Brun and F. Rademakers, Nucl. Instr. Meth. Phys. Res. **A** 389, 81 (1997).
[7] J. Cvach *et al.*, Proceeding of International Workshop on Future Linear Colliders (LCWS14), 9 pp, arXiv:1503.06940 [physics.ins-det] (2015).
[8] We used eight experimental (type A and type B) and four commercially available SiPMs (S12571) without trenches and two experimental (LCT4) and four commercially available SiPMs (S13360) with trenches from Hamamatsu photonics: http://www.hamamatsu.com/.
[9] We used two experimental (W12) and six commercially available SiPMs (PM3350) from KETEK GMBH: https://www.ketek.net/.
[10] We used four SiPMs from the Center for Prospective Technologies & Apparatus (CPTA). Joint venture with Photonique SA, www.photonique.ch.